Radius dependence of the melting temperature of single-walled carbon nanotubes: molecular-dynamics simulations

Radius dependence of the melting temperature of single-walled carbon nanotubes: molecular-dynamics simulations

Y Kowaki[1]**, A Harada**[1]**, F Shimojo**[2] **and K Hoshino**[1]

[1] Graduate School of Integrated Arts and Sciences, Hiroshima University, Higashi-Hiroshima 739-8521, Japan
[2] Graduate School of Science and Technology, Kumamoto University, Kumamoto 860-8555, Japan

E-mail: khoshino@hiroshima-u.ac.jp

Abstract

We have investigated the radius dependence of the melting temperature of single-walled carbon nanotubes (SWCNTs) by classical molecular-dynamics (MD) simulations using the environment-dependent interatomic potential (EDIP) proposed by Marks. Here we define the 'melting temperature' as a temperature at which there occurs a thermal instability of SWCNTs. We have carried out molecular-dynamics simulations at several temperatures for carbon nanotubes with various radii and estimated the 'melting temperature' based on the temperature dependence of the radial distribution functions, mean-square displacements and atomic configurations. It is shown that the 'melting temperature' of SWCNTs decreases with decreasing radius. The origin of this radius dependence of the melting temperature of SWCNTs is discussed in relation to the stability of SWCNTs energetically based on the strain energy of carbon nanotubes.

(Some figures in this article are in colour only in the electronic version)

1. Introduction

Since carbon nanotubes were discovered by Iijima [1], various properties such as the mechanical and electronic properties have been studied extensively both experimentally and theoretically [2]. Though their mechanical instability with respect to the external force has been studied widely (see [3] and references therein), to our knowledge, there have so far been few studies on the thermal instability or melting of carbon nanotubes.

As in previous studies on the thermal stability of carbon nanotubes, we quote the following two papers. Sun *et al* [4] discussed the thermal stability and determined the dimension and strength of a C–C bond in a single-walled carbon nanotube (SWCNT) based on the known

product of Young's modulus Y and the wall thickness t ($Yt \simeq 0.3685$ TPa nm) and the known tip-end and tube-wall melting temperatures, 1593 and 1605 K respectively, as well as their functional dependence on atomic coordination and bonding energy. López *et al* studied the structural and thermal stability of narrow and short carbon nanotubes and nanostrips by molecular-dynamics (MD) simulation using the Tersoff potential [6, 7]. They studied the relative stability of narrow finite length SWCNTs and nanostrips as a function of their length and found that the critical radius ($\sim$0.2 nm) for tube stability is independent of the length of the tubes and the chirality. They also found that the strips exhibit a higher thermal stability than the tubes even in those cases where they are structurally less stable and the thermal decomposition temperature ($\sim$1000 K) of the tubes comes out in good agreement with the experiments.

In the previous studies, the thermal stability was discussed in terms of the 'melting temperature', which was defined to be the temperature at which the bond breaking starts. In this paper we define the '*melting temperature*' T_m as a temperature at which a thermal instability of SWCNTs occurs, i.e. the breakdown of the nanotube. Therefore, our definition of the 'melting temperature' is different from that of the previous one, and the former and the latter should be considered as the upper and lower bound, respectively. It should be noted that, strictly speaking, we are not concerned with the melting phenomenon, which is a first-order solid–liquid phase transition. We are just investigating the thermal instability of carbon nanotubes.

Since the melting temperature of graphite is 4700–4900 K, which depends on the pressure [8, 9], the melting temperature of carbon nanotubes is expected to be about 5000 K and may depend on the size or radius of the carbon nanotubes. Because of its high temperature, it is difficult to obtain the melting temperature experimentally and therefore it is useful and meaningful to study the thermal instability of carbon nanotubes by computer simulations. So far some empirical interaction potentials such as Tersoff [6, 7] and Brenner [10] potentials have been widely used in the simulation for carbon systems. In this study we employ the environment-dependent interaction potential (EDIP) proposed by Marks [11]. The EDIP was originally proposed by Justo *et al* [12] for silicon, and then extended to carbon by Marks. Marks introduced the generalized coordination functions, parametrized using *ab initio* data, which describe dihedral rotation, nonbonded π-repulsion and fractional coordination, and showed that simulations of liquid carbon compare very favourably with *ab initio* MD simulations and that amorphous networks generated by quenching the liquid have properties superior to those obtained by the Tersoff and Brenner potentials. In the simulation by Marks, the liquid structure at 5000 K was studied and the results agreed with those of *ab initio* Car–Parrinello simulations. The present authors have also studied the dynamic as well as static structures of liquid carbon at 5000 K, using both classical MD simulation with EDIP and *ab initio* MD simulations, and showed that the results obtained by these methods agree well [13, 14]. Therefore we can conclude from these comparative studies that the EDIP for carbon proposed by Marks can describe various states of carbon systems including high-temperature liquids. These are reasons why we employ the EDIP proposed by Marks in this study.

The purposes of this paper are (i) to investigate the radius dependence of the melting temperature of SWCNTs by classical MD simulations using the EDIP proposed by Marks [11] and (ii) to discuss the physical origin of its radius dependence.

2. Method of calculation

2.1. Model

Our model systems are armchair-type SWCNTs with chiral vectors (5, 5), (7, 7), (10, 10), (12, 12), (15, 15) and (20, 20), which correspond to the radii from 0.343 to 1.38 nm. The nearest-

neighbour distance between carbon atoms is taken to be 0.142 nm, which is the bond length of graphite. We consider SWCNTs with infinite length along the z axis. Therefore we take from 240 to 960 carbon atoms in our unit cell $L_x \times L_y \times L_z$, where $L_x(L_y, L_z)$ is the length of a unit cell in the $x(y, z)$ direction, and impose periodic boundary conditions along the x-, y- and z-directions. To avoid the interaction between carbon nanotubes, we take L_x and L_y large enough, i.e. $L_x = L_y = 2.54$–6.35 nm, where L_z is fixed to be 2.95 nm.
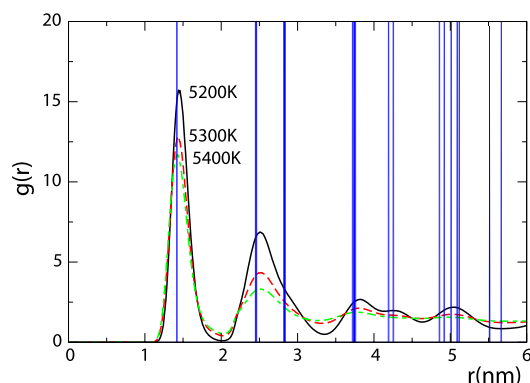
2.2. Method of simulation

We carry out constant-temperature classical MD simulations for our model systems using the EDIP proposed by Marks [11] and Nosé–Hoover thermostat for the temperature control. The cutoff distance of the interatomic force derived from the EDIP is taken to be 0.32 nm. In this paper, we employ the classical MD simulation, since there exist reasonably good interatomic interaction potentials for carbon and we need to treat large number of atoms to investigate the radius dependence of T_m. The EDIP is designed so as to describe the sp^2 and sp^3 bondings as well as the π bonding and it has been shown that the EDIP succeeds in describing the static and dynamical structures of liquid and amorphous carbon systems, where various local atomic configurations arise, and a graphene sheet [11, 13, 14]. Though, in the case of flat two-dimensional graphene, the bonding between carbon atoms is mainly determined by the sp^2 and π bondings, it is not the case for carbon nanotubes since the wrapping of graphene results in a curved surface, where the bonding between carbon atoms cannot be described only by sp^2 and π bondings. Since it has been shown that the EDIP can describe the bonding between carbon atoms for a wide range of atomic configurations, we consider that the EDIP can also describe carbon nanotubes with various radii.

　　We carry out MD simulations for six model carbon nanotubes with different radii. At each temperature we carry out MD simulations for 23 000 steps with a time step $\Delta t = 0.6$ fs and calculate physical quantities using last 20 000 steps, where the first 3000 steps are used for thermal equilibration. We start our MD simulations for initially perfect SWCNTs and then increase the temperature with an increment of 100 K until the system shows thermal instability. We repeat this procedure for all model systems with different radii and obtain the radius dependence of the melting temperature of SWCNTs.

2.3. Criteria for determining the melting temperature of SWCNTs

As mentioned in section 1, we define the '*melting temperature*' T_m as a temperature at which there occurs a thermal instability of SWCNTs when the temperature is increased. As for the criteria for the thermal instability, we use the temperature dependences of the radial distribution function $g(r)$, the mean-square displacement (MSD) and the atomic configuration. Since we start our MD simulations with the perfect SWCNT, where the sharp peaks of $g(r)$ correspond to the periodic atomic configuration of the SWCNT, the peaks of $g(r)$ become broader due to thermal effects with increasing temperature and the peaks corresponding to third neighbours and beyond tend to disappear when the temperature is higher than the instability temperature T_m. As for the MSD as a function of time, we can observe a large increase of the gradient of the curve, which corresponds to the diffusion coefficient, for $T > T_m$. These features suggest thermal instability of SWCNTs and we confirm this fact by the temperature dependence of the atomic configuration as a function of time.

　　It should be noted that, since our simulation time is finite, it may be possible that longer simulations may give rise to lower T_m. In this sense, our T_m should be considered as the upper bound of T_m.

Figure 1. The temperature dependence of the radial distribution function $g(r)$ of SWCNTs with chiral vector (10, 10) and radius of 0.682 nm. The sharp peaks correspond to the first-, second-, third- and so on neighbours of perfect SWCNTs, which is the initial configuration of our MD simulation. There occurs a qualitative change in $g(r)$ between 5200 and 5300 K.

3. Results and discussion

3.1. Radial distribution function g(r)

We show in figure 1 the temperature dependence of $g(r)$ for SWCNTs with chiral vector (10, 10) and a radius of 0.682 nm. The sharp peaks correspond to the first-, second-, third- and so on neighbours of perfect SWCNTs, which is the initial configuration of our MD simulation. As seen from this figure, with increasing temperature, the peaks of $g(r)$ corresponding to the intermediate correlation, i.e. the peaks of third-, fourth- and beyond, become broader at first and then change qualitatively, namely the peaks disappear, for temperatures $T > T_m$, where T_m is estimated to be about 5250 K from figure 1. We have carried out MD simulations for 20 000 time steps at each temperature with an increment of 100 K.
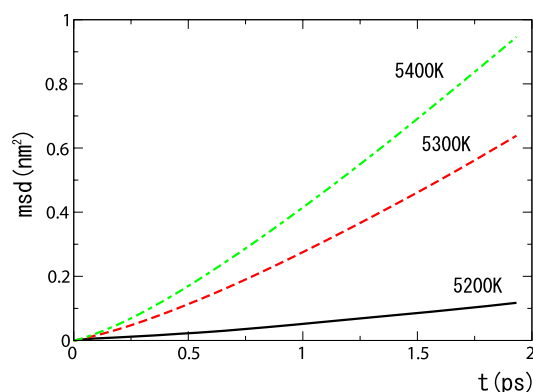
We repeated this procedure of simulations for six model SWCNTs with different chiral vectors to estimate their melting temperatures.
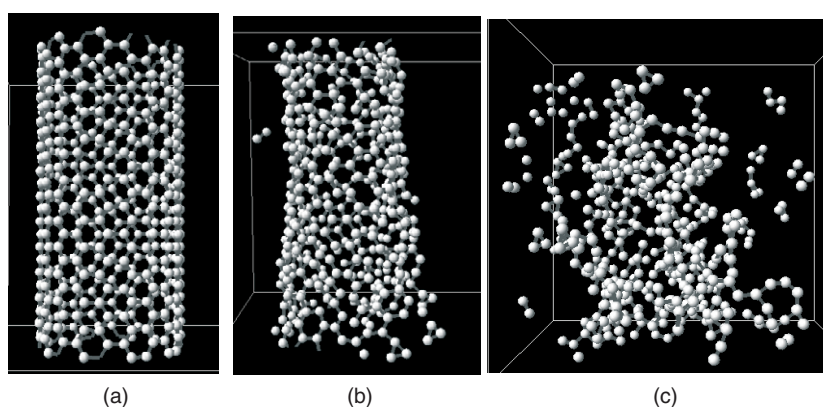
3.2. MSD

In figure 2 we show the MSD as a function of time t for an SWCNT with chiral vector (10, 10) and a radius of 0.682 nm at three temperatures. It is known that the MSD $= 6Dt$ for large t, where D is the self-diffusion coefficient. It is seen from figure 2 that the MSD curves for $T > T_m = 5250$ K correspond to non-crystalline systems, in the sense that the values of D estimated from the gradients of these MSD versus t curves for $T > T_m$ are of the order of 10^{-4} cm^2 s^{-1}, which is an order of magnitude of D for typical liquids.

3.3. Atomic configuration

We show in figures 3(a)–(c), the atomic configurations of SWCNTs with chiral vector (10, 10) and radius of 0.682 nm (a) for the initially perfect SWCNT, (b) for $T = 5200$ K $< T_m$ after 20 000 time steps and (c) for $T = 5300$ K $> T_m$ after 20 000 time steps, respectively. It is clearly seen from (b) and (c) that the SWCNT for (b) remains as a distorted tube, though the SWCNT for (c) cannot sustain its tubular shape, i.e. the breakdown of the carbon nanotube. In these figures we show snapshots of atomic configurations, within a unit cell, though our

Figure 2. The temperature dependence of the MSD of SWCNTs with chiral vector (10, 10) and radius of 0.682 nm.
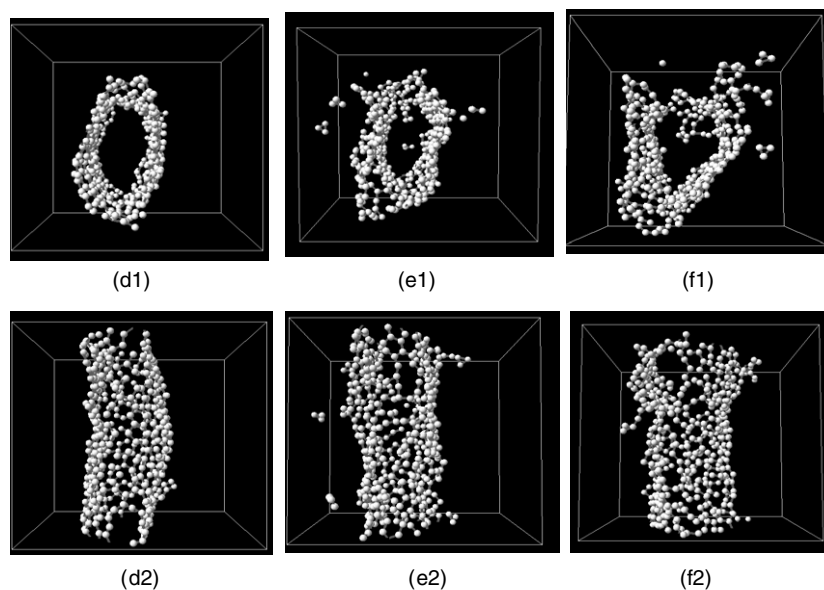

(a)   (b)   (c)

Figure 3. The atomic configurations (a) for the initially perfect SWCNT, (b) for $T = 5200$ K $< T_m$ after 20 000 time steps and (c) for $T = 5300$ K $> T_m$ after 20 000 time steps, respectively.

SWCNT is an infinite-length system. In these figures we connect by bonds two carbon atoms nearer than the cutoff distance of 0.16 nm, which is taken to be a little bit longer than the nearest-neighbour distance, 0.142 nm, of the graphite crystal.
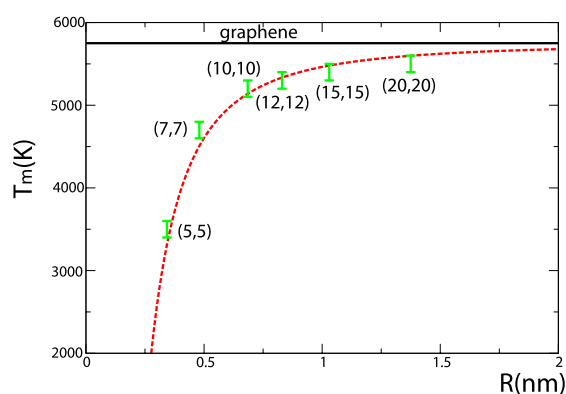
In figures 4(d1)–(f1) and (d2)–(f2) we show the sequence of snapshots of atomic configurations for $T = 5300$ K $> T_m$ at (d) 6500, (e) 8500 and (f) 10 100 time steps, viewed from the z-direction (along the tube axis, i.e. 'the top view') and from the x, y-direction (perpendicular to the tube axis, i.e. 'the side view'), respectively. From figures 4(d1)–(f1) and (d2)–(f2), we can see the dynamical process of the breakdown of carbon nanotubes. Breaking and rearrangement of C–C bonds occur due to thermal fluctuation and then the nanotube breaks down, i.e. the tubular shape disappears. We can see from the top view of the nanotube that the shape of the cross section of the nanotube changes as a function of time and deforms from a circle to an oval (see figure 4(d1)) due to the thermal fluctuation.

3.4. Radius dependence of the melting temperature of SWCNTs

We have estimated the 'melting temperatures T_m' of SWCNTs from the temperature dependences of $g(r)$, MSD and atomic configurations and show T_m in figure 5 as a function
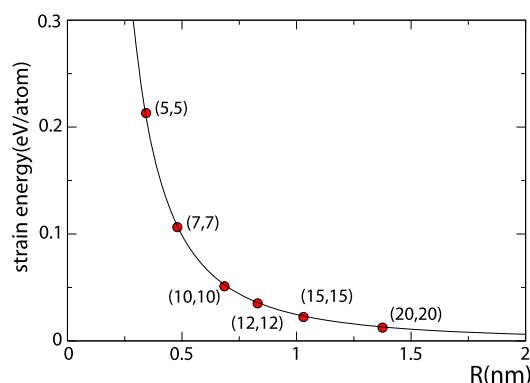
Figure 4. The atomic configurations for $T = 5300$ K $> T_m$ at (d) 6500, (e) 8500 and (f) 10 100 time steps, respectively. Here (d1), (e1), (f1) and (d2), (e2), (f2) show the top and side views, respectively.

Figure 5. The radius dependence of the melting temperature T_m of SWCNTs, which are estimated from the temperature dependences of $g(r)$, MSD and atomic configurations. The T_m of a graphene estimated in the same way, 5750 K, is also shown by a horizontal line. The broken curve shows the T_m given by the relation described in section 3.6.

of the radius R of SWCNTs. We have applied the same method to a sheet of graphite, i.e. a graphene. The T_m of graphene thus estimated is 5750 K and is also shown in figure 5. We can see from this figure that the T_m of SWCNTs (i) decreases with decreasing radius and (ii) approaches that of graphene with increasing radius. The characteristic feature (ii) is natural, since the SWCNT approaches the graphene in the limit of $R \to \infty$. We show the error bars in figure 5, since we carried out our MD simulation at temperatures with an increment of 100 K. The origin of this radius dependence of T_m of SWCNTs is discussed below.

Figure 6. The strain energy of SWCNTs as a function of radius. The solid curve is C/R^2, where $C = 24.7$ meV nm^2 to fit our MD results.

We should mention here about the reason for the difference in the melting temperature obtained by us and others [4, 5]. The reasons are as follows. (i) Our model SWCNT is an infinite-length tube and there is no 'tip-end', since we are imposing the periodic boundary condition. Therefore there is no tip-end melting in our model. The tip-end melting temperature should be lower than the 'bulk' (infinite length) melting temperature. (ii) Our definition of 'melting' is different from previous studies: we define the melting of SWCNTs by the temperature at which the thermal instability of nanotubes occurs, i.e. the breakdown of the nanotube, while others define it by the temperature at which the bond breaking starts. Obviously the former (upper bound) is higher than the latter (lower bound).

As far as we have investigated, our melting temperature for an infinite graphite sheet, so-called graphene, is about 5800 K. This is higher than the T_m of bulk graphite, since the interactions between graphite layers are weak van der Waals like ones, though the C–C bonds within the layers are very strong sp^2 covalent bonds. Therefore the layer structure of graphite breaks down at a lower temperature than the layer itself does.

As shown here, the T_m of SWCNTs is lower than the graphene $T_m^{graphene}$ and decreases as $T_m^{graphene} - $ constant$/R^2$ (R: radius of SWCNT), which comes from the R-dependence of the strain energy of SWCNTs as will be discussed in the following.

3.5. Strain energy of SWCNTs

We show in figure 6 the strain energy or the curvature energy of SWCNTs as a function of radius. Here the '*strain energy*' is defined by the difference of the potential energy of SWCNTs and that of a graphene, i.e. the potential energy per atom of SWCNTs relative to that of a graphene. In figure 6 the solid curve is C/R^2 and the fitted value of C to our results of MD simulations using EDIP is 24.7 meV nm^2. It has been shown by various theories [15–17, 3, 18] that the strain energy can be written as C/R^2. The values of C estimated are 20.0 meV nm^2 from classical elastic theory [15], and 20.5 [16], 21.2 [17] and 19.6 meV nm^2 [3] from *ab initio* MD simulations. The classical MD simulations using Tersoff and Tersoff–Brenner potentials give $C = 15$ and 12 meV nm^2 [18], respectively. The value of C estimated by our classical MD simulation using EDIP is in reasonable agreement with those estimated by previous theoretical studies.

With decreasing radius of SWCNT, the bond angles of SWCNTs deviate from 120°, which corresponds to the bond angle of sp^2 bonding, and decrease as was shown by previous

studies [16]. This means that, with decreasing radius of SWCNT, the bonding between carbon atoms is not purely sp^2 bonding but a mixture of sp^2 and sp^3 bondings. The latter is energetically higher than the former. This is the origin of the strain energy or the curvature energy and can be considered as the wrapping effect on carbon nanotubes.

3.6. Origin of the radius dependence of T_m of SWCNT

In general, the melting temperature is correlated to the strength of bonding between atoms in crystals, in other words, to the stability of the crystal. Therefore we can understand the radius dependence of the melting temperature of SWCNTs shown in figure 5 on the basis of the radius dependence of the strain energy of SWCNTs shown in figure 6. That is, when the strain energy becomes larger, the melting temperature becomes lower.

As mentioned above, the strain energy E_{strain} is defined by

$$E_{\text{strain}} = E_{\text{pot}}^{\text{SWCNT}} - E_{\text{pot}}^{\text{graphene}}, \tag{1}$$

where $E_{\text{pot}}^{\text{SWCNT}}$ and $E_{\text{pot}}^{\text{graphene}}$ are the potential energies of the SWCNT and a graphene, respectively, and these can be considered as -(binding energy) or -(cohesive energy). Since the binding energy is strongly correlated to the melting temperature, we can write

$$E_{\text{strain}} \sim -k_{\text{B}} T_{\text{m}}^{\text{SWCNT}} - (-k_{\text{B}} T_{\text{m}}^{\text{graphene}}), \tag{2}$$

where $T_{\text{m}}^{\text{SWCNT}}$ and $T_{\text{m}}^{\text{graphene}}$ are, respectively, the melting temperature of the SWCNT and a graphene, and k_{B} is the Boltzmann constant. Therefore we have a relation

$$T_{\text{m}}^{\text{SWCNT}} - T_{\text{m}}^{\text{graphene}} \sim -E_{\text{strain}}/k_{\text{B}} = -(C/k_{\text{B}})/R^2. \tag{3}$$

In figure 5, the relation, $T_{\text{m}}^{\text{SWCNT}} - T_{\text{m}}^{\text{graphene}} = -E_{\text{strain}}/k_{\text{B}} = -(C/k_{\text{B}})/R^2$, is shown by a broken curve. As is seen from this figure, the relation can describe the radius dependence of T_{m} semi-quantitatively. Therefore T_{m} of the SWCNT decreases in proportion to $-1/R^2$.

The radius dependence of the melting temperature of a SWCNT is phenomenologically similar to that of the fine particles [19, 20]. The origin of the radius dependence, however, is physically different. In the case of fine particles, the ratio of the number of surface atoms to the number of total atoms in a fine particle increases with decreasing radius R of fine particles in proportion to $1/R$ and the surface atoms are less stable than bulk atoms in the sense that the former atom is surrounded by a smaller number of atoms than the latter. On the other hand, the SWCNT is composed of a curved or wrapped graphene sheet, where all atoms belong to the surface, and the SWCNT with smaller radius has larger strain energy. Therefore the SWCNT with smaller radius is less stable energetically and the thermal instability occurs at lower temperature, which is the origin of the radius dependence of the melting temperature shown in figure 5.

4. Conclusion

We have applied the constant-temperature classical MD simulation to the model systems for infinite-length single-walled carbon nanotubes with various radii to investigate the radius dependence of the '*melting temperature*' T_{m}, which is defined as the temperature at which thermal instability occurs in SWCNTs; T_{m} is obtained from the temperature dependences of $g(r)$, MSD and atomic configurations. We have found that the T_{m} decreases as the radius of SWCNT decreases. The origin of this behaviour is correlated to the radius dependence of the strain energy of SWCNTs, on which the stability of SWCNTs depends. The larger the strain energy is, the lower the melting temperature is.

Acknowledgments

References

[1] Iijima S 1991 *Nature* **354** 56
[2] Saito R, Dresselhaus G and Dresselhaus M S 1998 *Physical Properties of Carbon Nanotubes* (London: Imperial College Press)
[3] Hasegawa M and Nishidate K 2006 *Phys. Rev.* B **74** 115401
[4] Sun C Q, Bai H L, Tay B K, Li S and Jiang E Y 2003 *J. Phys. Chem.* B **107** 7544
[5] López M J, Cabria I, March N H and Alonso J A 2005 *Carbon* **43** 1371
[6] Tersoff J 1988 *Phys. Rev. Lett.* **61** 2879
[7] Tersoff J 1988 *Phys. Rev.* B **37** 6991
[8] Togaya M 1997 *Phys. Rev. Lett.* **79** 2474
[9] Savvatimskiĭ A I 2003 *Phys.—Usp.* **46** 1295
[10] Brenner D W 1990 *Phys. Rev.* B **42** 9458
[11] Marks N A 2001 *Phys. Rev.* B **63** 035401
[12] Justo J F, Bazant M Z, Kaxiras E, Bulatov V V and Yip S 1998 *Phys. Rev.* B **58** 2539
[13] Harada A, Shimojo F and Hoshino K 2003 *J. Phys. Soc. Japan* **72** 822
[14] Harada A, Shimojo F and Hoshino K 2005 *J. Phys. Soc. Japan* **74** 2270
[15] Tibbetts G G 1984 *J. Cryst. Growth* **66** 632
[16] Sánches-Portal D, Artacho E, Soler J M, Rubio A and Ordejón P 1999 *Phys. Rev.* B **59** 12678
[17] Adams G, Sankey O, Page J, O'Keeffe M and Drabolt D 1992 *Science* **256** 1792
[18] Robertson D H, Brenner D W and Mintmire J W 1992 *Phys. Rev.* B **45** 12592
[19] Hoshino K and Shimamura S 1979 *Phil. Mag.* A **40** 137
[20] Hasegawa M, Hoshino K and Watabe M 1980 *J. Phys. F: Met. Phys.* **10** 619